

Enhancement of Shock-to-Detonation Transition in Channels with Regular Shaped Obstacles

Sergey M. Frolov¹, Ilya V. Semenov², Pavel S. Utkin², Pavel V. Komissarov¹,
Vladimir V. Markov³

¹N.N. Semenov Institute of Chemical Physics,
Russian Academy of Sciences, Moscow 119991, Russia

²Institute for Computer Aided Design,
Russian Academy of Sciences, Moscow 123056, Russia

³V.A. Steklov Mathematical Institute,
Russian Academy of Sciences, Moscow 119991, Russia

1 Introduction

Recent review [1] of experimental studies on gaseous and spray detonation initiation by a traveling ignition source indicates that spatially distributed electric dischargers with properly tuned triggering times provide very short distances for shock-to-detonation transition (SDT) in a smooth-walled tube. According to [1], available experiments on deflagration-to-detonation transition (DDT) in tubes with regular or irregular obstacles [2] can also be treated as detonation initiation by a traveling ignition source. In this case, instead of external stimulation of chemical activity behind a propagating shock wave, a localized obstacle-induced autoignition of shock-compressed gas occurs which is closely coupled to the shock wave intensity and compression phase duration. In terms of the ignition delay, the conditions for the coupling between mixture autoignition and the propagating shock wave seem to be equivalent to those found in the experiments with external energy deposition using spatially distributed electric discharges. In case the ignition timing at obstacles is closely coupled with the propagating shock wave, favorable conditions for ‘fast’ DDT can occur [1]. Otherwise, the propagating shock wave decouples from the ignition pulses and DDT fails or occurs at a later stage due to cumulating of flame-induced pressure waves and “explosion in the explosion” phenomenon. The latter DDT scenario was referred in [1] to as ‘slow’ DDT.

With this understanding of the DDT phenomena, new approaches to reducing the predetonation distance for pulse detonation engine (PDE) applications can be considered. One of such approaches is suggested in this paper. The underlying idea is to promote fast DDT by appropriate shaping of regular obstacles in the detonation tube. It is implied that shock-induced autoignition of the reactive mixture at the obstacles and hence the shock wave – reaction front interaction can be efficiently controlled not only by obstacle blockage ratio and spacing, but also by obstacle shape due to gasdynamic focusing of the propagating shock wave. Note that the focusing effect of regular shaped obstacles in the tube on shock wave propagation in reactive media has not hitherto been studied, although the phenomenon of shock wave focusing in straight tubes after reflection from a nonflat end wall has long been known.

2 Computational study

Among different shapes of obstacles, orifice plates and combinations of parabolas were chosen for consideration in this study [3]. Regular orifice plates were taken as an example of obstacles used in the majority of available DDT studies. Their performance as DDT enhancing elements was compared with the performance of regular obstacles shaped as shown in Fig. 1. The obstacles of Fig. 1 were composed of two parabolas x_1 and x_2 with the identical focal point F lying at the symmetry plane of the 2D channel of height H . The obstacle contours are depicted by solid curves, so that points A and B correspond to obstacle vertices. Obstacle height is denoted as h . In general, coefficients a_1 , b_1 , and c_1 can differ from coefficients a_2 , b_2 , and c_2 , and the focal points of parabolas x_1 and x_2 do not coincide. Similar obstacles were positioned in the channel at a distance between vertices $\delta = x_1(0) - x_2(0)$ thus forming a regular array of shaped obstacles. The total length of the channel section with regular obstacles was L . To the left and to the right of the obstructed section, a provision

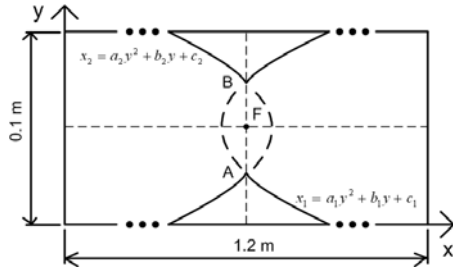


Fig. 1: Schematic of shaped parabolic obstacles in the 2D channel

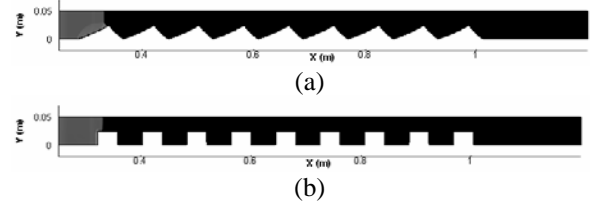


Fig. 2: Shock wave enters the channel section with regular shaped obstacles (a) and with orifice plates (b)

was made for smooth initiation and outlet channel sections of height H and lengths L_- and L_+ . For the sake of comparison, regular rectangular obstacles were used. In this case, the height h and the total cross-section area of the obstacles in the x - y plane were kept similar to the corresponding case with the shaped obstacles. It was assumed that initially the channel was filled with a quiescent, premixed, explosive gas at temperature T_0 and pressure p_0 . A planar shock wave of initial Mach number M and compression phase duration τ was generated in the initiation section and, propagating from left to right, entered the obstructed section of the channel (Fig. 2). In the obstructed section, ignition of the explosive gas caused by shock wave reflections from the obstacles and interactions between various wave systems could occur.

After ignition, two scenarios of the post-shock flow evolution leading to SDT can be considered. In the first, turbulent flame kernels develop in the channel, giving rise to combustion-generated compression waves catching up with the lead shock wave. In the long run, the “explosion in the explosion” phenomenon can occur in the region between the turbulent flame brush and the lead shock wave. In the second, the stage of turbulent flame development and propagation is of minor importance as compared to fast energy deposition in the spontaneous ignition fronts propagating in the portions of explosive gas preconditioned by multiple shock compression. This study is focused on the second scenario.

The mathematical model used was based on the full 2D Navier – Stokes equations supplemented by the equation of energy conservation, equation of chemical kinetics, and the ideal gas equation of state. The chemical transformation in the mixture was modeled by a single-step chemical reaction with the Arrhenius expression for the reaction rate calibrated for a particular fuel – air mixture in terms of the high-temperature ignition delays. Since the primary focus of this study is the fast SDT due to spontaneous ignitions governed by shock reflections, no turbulence and turbulent combustion models were involved. The numerical procedure was similar to that reported in [3]. It was based on the finite volume approach and Godunov flux approximation and was implemented for parallel computing.

The problem was solved for the lower part of the channel of Fig. 1 with the symmetry boundary conditions at the symmetry plane. The explosive gas was the stoichiometric propane–air mixture at normal initial conditions. The geometrical dimensions of the channel were: $L_- = 0.25$ m, $L = 0.76$ m, $L_+ = 0.19$ m, and $H = 0.1$ m. The initial parameters of the shock wave were: $M = 3$ and $\tau \approx 800 \mu\text{s}$. The shock wave was generated by a high-pressure domain L_- filled initially with air at $T_- = 1159$ K and $p_- = 6.06$ MPa. The only parameters varied in this study were the parameters determining the obstacle shape. A fine (unstructured) computational grid with 200 000 cells was used. The spatial resolution was about $100 \mu\text{m}$ and the maximal time step was 10 ns.

The optimal obstacle shape for the conditions outlined above was obtained in the course of the special optimization study. The parabolic obstacle height was $h = 0.025$ m. The coordinate of obstacle focus was $x = 0.065$ m, $y = 0.05$ m, $c_1 = 0.08$ m, $c_2 = 0$ m. The total number of obstacles at length L was 9. Figure 3 shows the predicted snapshots of the temperature field in the channel with regular parabolic obstacles. At about $490 \mu\text{s}$ (snapshot 1), spontaneous ignition occurred above the fifth obstacle in the vicinity to the focal point, which gave rise to a detonation. The detonation wave passed the obstructed section of the channel and propagated steadily in the smooth outlet section. When the initial shock wave entered the obstructed section from the right end, with other conditions being identical to those for Fig. 3, no SDT was detected in the calculations. This test indicates the importance of the upwind and wake shapes of the regular obstacles. Similar calculations for the channel with

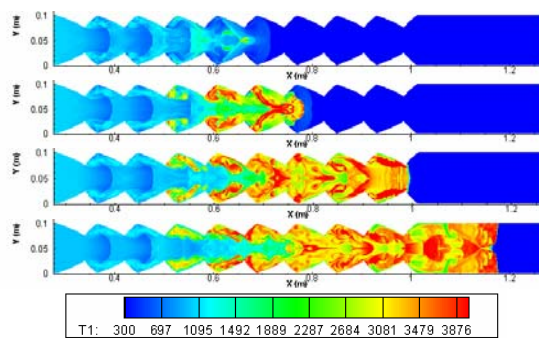


Fig. 3: Snapshots of temperature fields at SDT in the channel with regular parabolic obstacles. The upper snapshot corresponds to $480 \mu\text{s}$. Other snapshots are plotted with the time interval of $100 \mu\text{s}$

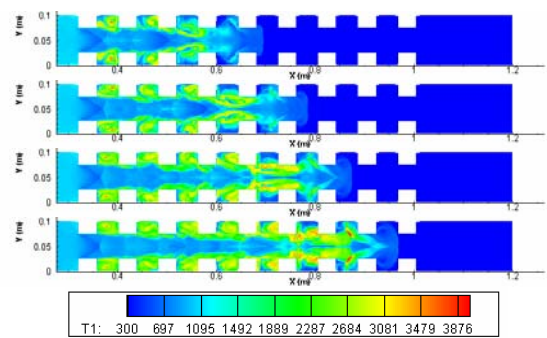


Fig. 4: Snapshots of temperature fields in the channel with regular orifice plates. The upper snapshot corresponds to $480 \mu\text{s}$. Other snapshots are plotted with the time interval of $100 \mu\text{s}$

9 rectangular obstacles of the same height $h = 0.025$ m and pitch $\delta = 0.08$ m did not result in the detonation onset. Figure 4 shows the corresponding predicted snapshots of the temperature field in the channel with regular rectangular obstacles. Despite earlier ignition as compared to Fig. 3, the rectangular obstacles did not promote fast SDT. Only with the initial shock of Mach number exceeding 3.5 it was possible to initiate detonation in the channel with regular rectangular obstacles.

For better understanding the SDT phenomenon in the channel with regular parabolic obstacles, we studied carefully the preignition spatial temperature distributions in the vicinity to the ignition site above the fifth obstacle in Fig. 3. A large mixture volume (about 10 mm long and 3 mm wide) with the temperature exceeding 2000 K was found to exist in this region. The temperature distribution in this volume was not homogeneous: there were two islands with the maximal temperatures of 2250 K and 2100 K separated with a narrow “strait” with the temperature of 2050 K. The islands were oriented streamwise but were shifted both horizontally and vertically with respect to each other. Analyzing the results of calculations, we found that the reaction front propagated exactly along this preconditioned volume, giving rise to a strong secondary blast wave. After reflection of this blast wave from the fifth obstacle, a detonation bubble formed. These observations testify that the detonation forms due to spontaneous generation of a strong blast wave in the exothermic center. The mechanism of blast wave formation due to propagation of fast spontaneous flames in the compressible medium was studied elsewhere [4].

3 Experimental study

The new approach to reduce the predetonation distance using shaped regular obstacles in the detonation tube was validated experimentally. Figure 5 shows the schematic of the experimental setup. The setup contained a high-pressure chamber (HPC) to generate shock waves of different initial intensity and a low-pressure chamber (LPC) with the obstructed section possessing two rectangular (350x110 mm) optical windows. The total length of the tube was 2.5 m. The HPC was initially separated from the LPC by the bursting diaphragm. The obstructed section was 100x100 mm square channel 1 m long with the regular obstacles. This section reproduced exactly the shapes and arrangements of the parabolic and rectangular obstacles of Figs. 3 and 4. The experiments were made with the stoichiometric propylene–air mixture at normal initial conditions. The shock waves were generated by filling the HPC (up to 8 bar) with the stoichiometric propylene–oxygen mixture and igniting it with a standard spark plug. The reactive mixtures were prepared by partial pressures in two mixers. Before each run, the LPC was purged by about 5 volumes of the reactive mixture. To register the propagation velocities of shock waves and detonations, 6 high-frequency pressure transducers were installed along the tube (circular dots in Fig. 5). The data acquisition system comprised an analog-to-digital converter (100 kHz per channel) and a PC. The measuring errors of shock wave velocity and pressure was estimated as 3% and 30%, respectively. For visualizing shock-induced ignition and reaction front propagation, a CCD videocamera VS-Fast (5000 frame/s) was used. The pressure records of the SDT in the tube with parabolically-shaped regular obstacles are shown in Fig. 6. Figure 7 shows the pressure records obtained in the tube with rectangular-shaped regular obstacles at the.

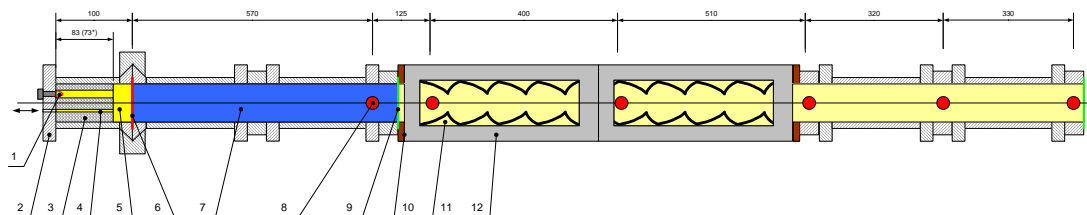


Fig. 5: Schematic of the experimental setup

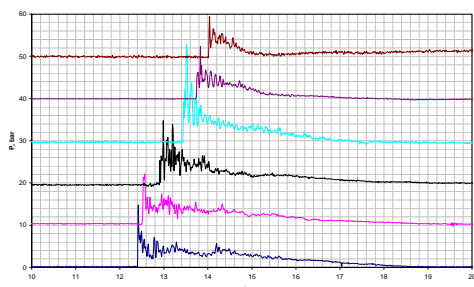


Fig. 6: Pressure records in the tube with parabolic obstacles in the stoichiometric propylene–air mixture. The initial shock wave velocity is 1070 ± 30 m/s

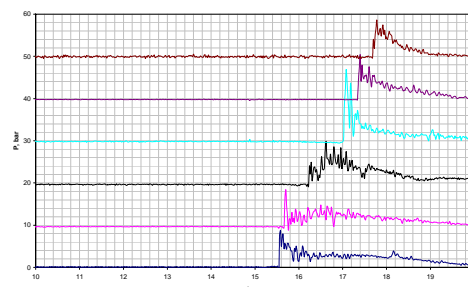


Fig. 7: Pressure records in the tube with rectangular obstacles in the stoichiometric propylene–air mixture. The initial shock wave velocity is 1070 ± 30 m/s

Table 1: Comparison of measured shock wave velocities in the tube with regular parabolic and square obstacles

Measuring segment, mm	Shock wave velocity, m/s	
	parabolic	rectangular
670-795	1070 ± 30	1070 ± 30
795-1195	1061 ± 30	714 ± 20
1195-1705	836 ± 25	637 ± 20
1705-2025	1025 ± 30	1000 ± 30
2025-2355	1590 ± 50	970 ± 30

the same initial shock wave velocity. Table 1 shows the corresponding data for the two sets of experiments with parabolic and rectangular obstacles at identical initial conditions. Clearly, parabolic obstacles promoted SDT whereas the use of rectangular obstacles did not result in the detonation onset.

Concluding remarks

The results of numerical simulation of SDT in the channel with regular obstacles indicate that proper obstacle shaping can be used for a considerable reduction of the SDT distance and time for PDE applications. In the example considered, the SDT distance and time for the stoichiometric propane–air mixture was about 0.55 m and 490 μ s, respectively. The physical mechanism governing fast SDT is closely connected with explosive gas preconditioning by multiple shock compression in the vicinity to the focal points of the parabolic obstacles. The use of regular “unshaped” obstacles did not result in the SDT, other conditions being equal. Preliminary experiments with the stoichiometric propylene–air mixture confirmed these findings.

This study was partly supported by the ISTC (project #2740) and RFBR (grant #05-08-50115).

References

1. Frolov S. M. J. Loss Prevention, 2005, Vol 19/2-3, pp. 238-244.
2. Shchelkin, K. I., *Fast Combustion and Spinning Detonation of Gases*, Voenizdat, Moscow, 1949, pp. 44–73.
3. Semenov I., Frolov S., Markov V., Utkin P. In: Pulsed and Continuous Detonations. Ed. By G. Roy, S. Frolov, J. Sinibaldi. Moscow, Torus Press, 2006, pp. 159-169.
4. Gelfand B.E., Frolov S.M., Tsyganov S.A. Chemical Physics Reports, 1989, Vol. 8, No.5, pp. 1547-1553.